ELSEVIER

Polymer 43 (2002) 1615–1622

polymer

www.elsevier.com/locate/polymer

Studies on cross-linked polyurethane acrylate-based electrolyte consisting of reactive vinyl/divinyl diluents

M.L. Digar, S.L. Hung, T.C. Wen*, A. Gopalan[1]

Department of Chemical Engineering, National Cheng Kung University, Tainan 701, Taiwan, ROC

Received 13 July 2001; received in revised form 23 October 2001; accepted 25 October 2001

Abstract

A series of cross-linked polyurethane acrylate (PUA) electrolytes have been prepared by using 4,4′-methylene bis(phenyl isocyanate), polyethylene glycol, hydroxyethyl methacrylate and different reactive vinyl/divinyl diluents, such as methyl methacrylate (MMA), ethyl acrylate and acrylonitrile, tripropylene glycol diacrylate (TPGDA). The electrolytes were prepared by UV radiation induced cross-linking of the PUA–diluent mixture followed by swelling in a liquid electrolyte (LP-30). Depending upon the composition of the components, these electrolytes exhibited a wide range of mechanical and electrical properties. The system containing MMA as reactive diluent showed highest conductivity, but poor mechanical properties and stability in the liquid electrolyte. The TPGDA cross-linked system possesses a good combination of ionic conductivity and stability in liquid electrolytes. These systems showed good compatibility with Li-electrodes and sufficient electrochemical stability to allow safe operation in rechargeable Li-batteries.

Keywords: Polymer electrolyte; Polyurethane acrylate; Vinyl diluents

1. Introduction

Research effort has been very much focused to develop polymer electrolyte (PE) having combined high ionic conductivity and dimensional stability for use in rechargeable Li-batteries [1–3]. For battery applications, high ionic conductivity must be complemented by good dimensional stability since the PE will also function as separator in the battery providing electrical insulation between the anode and the cathode. Of the many polymers, polyethylene oxide (PEO) based electrolyte is the most widely studied. But the main drawback of PEO-based electrolyte is its low conductivity (10^{-8}–10^{-7} S/cm) at ambient temperature. The high degree of crystallinity of PEO, which is unfavorable for the mobility of the ions in the salt-doped PEO systems, restricts PEO to have conductivity. Several attempts have been made to obtain amorphous polyether matrices with high ionic conductivity over a wide temperature range [2,3].

Besides PEO, several alternative systems like poly (methyl methacrylate) (PMMA), poly(acrylonitrile) (PAN), poly(vinylidine fluoride) (PVdF), poly(vinyl chloride) (PVC), etc. have been investigated including thermoplastic polyurethane (TPU) [4–15]. The interest in using TPU as matrix for PE is related to the possibility of increasing mechanical strength of linear polyethers due to their phase-separated microstructure. The rubbery soft phase can dissolve alkali metal salts without formation of ionic clusters, which may be due to the interaction of ether oxygen with alkali metal ions [16,17]. Furthermore, the low glass transition temperature (T_g) and hence higher segmental motion of the polyether soft segments leads to higher mobility of the dissolved ions. The hard segment domains, which are in the glassy state and either distributed or interconnected throughout the rubbery phase of the soft segment, act as reinforcing filler and hence contribute to the dimensional stability of the PE.

Cross-linking of some of the units as side chains is one of the various ways to improve the mechanical properties of a polymer. It has been found that the comb-branched polymers based on phosphazene backbone and having PEO in the side chain are one of the highest conducting conventional PEs [18,19]. However, the mechanical properties of these systems are very poor due to the presence of flexible amorphous phase. In these systems, cross-linking with polyethylene glycol (PEG) [20] or by γ-ray induced cross-linking [21] results in dimensional stability. Cross-linked polymer networks prepared by radiation curing have

* Corresponding author. Tel.: +886-6-2385-487; fax: +886-6-2344-496.
E-mail addresses: tcwen@mail.ncku.edu.tw (T.C. Wen), algopal_99@yahoo.com (A. Gopalan).
[1] Permanent address: Department of Industrial Chemistry, Alagappa University, Karaikudi 630 003, India.

0032-3861/02/$ - see front matter
PII: S0032-3861(01)00737-6

received considerable attention in recent years. Radiation (UV) cured polyurethane acrylate (PUA) is one among them.

Velankar et al. [22] reported the UV curing of PUA oligomers. Although numerous studies have been done on the application of PUA in paints, coatings, inks, etc. [23], very few reports are available on their application in PEs. Recently, Kim et al. [24] reported the basic electrochemical properties of PUA–$LiCF_3SO_3$-based PEs by AC impedance measurements.

Present study directs its attention to find the effect of cross-linking PUA (based on 4,4′-methylene bis(phenyl isocyanate) (MDI), PEG and hydroxyethyl methacrylate (HEMA)) with different reactive diluents (vinyl and divinyl monomers) on the conductivity and electrochemical behavior of the electrolyte. The vinyl group of HEMA was effectively cross-linked with reactive diluents such as acrylonitrile (AN), or triphenyl glycol diacrylate or methyl methacrylate (MMA) or ethyl acrylate (EA) to generate the cross-linked PUA. The thermal behavior of the undoped and $LiClO_4$-doped cross-linked PUA systems was studied by thermogravimetric analysis (TGA) and differential scanning calorimetry (DSC).

2. Experimental

2.1. Materials

PEG (molecular weight = 1000; Showa) was dehydrated under reduced pressure at 80 °C for 24 h before use. MDI and HEMA (both Aldrich) were used as received. $LiClO_4$ (Aldrich) was dehydrated at 120 °C under reduced pressure for 72 h. The commercial battery electrolyte LP-30 (Merck) was used as received. This electrolyte is a 1 M solution of $LiPF_6$ in a 1:1 mixture of ethylene carbonate (EC) and dimethyl carbonate (DMC). Tripropylene glycol diacrylate (TPGDA), MMA, EA and AN were all from Aldrich and used without further purification. All other reagents and chemicals were used as received.

2.2. Synthesis of PUA

The PUA was synthesized by a two-step addition process, where the prepolymer was made by reaction of excess of MDI with PEG-1000 and then capping the end NCO groups by reaction with HEMA. The prepolymer was made by allowing the mixture of MDI and PEG-1000 to react at 60 °C for 2 h with constant stirring under a dry nitrogen blanket. After the prepolymer formation was over (confirmed by estimation of NCO groups by dibutyl amine back titration method), the temperature of the mass was reduced to 45 °C and then required amount of HEMA was slowly added to the reaction mixture. The reaction was allowed to continue for 3 h and then it was terminated by addition of ~0.2 g of methanol. The molar ratio of MDI, PEG and HEMA, maintained for making this PUA is 2:1:2. The structure of the synthesized PUA is shown in Fig. 1.

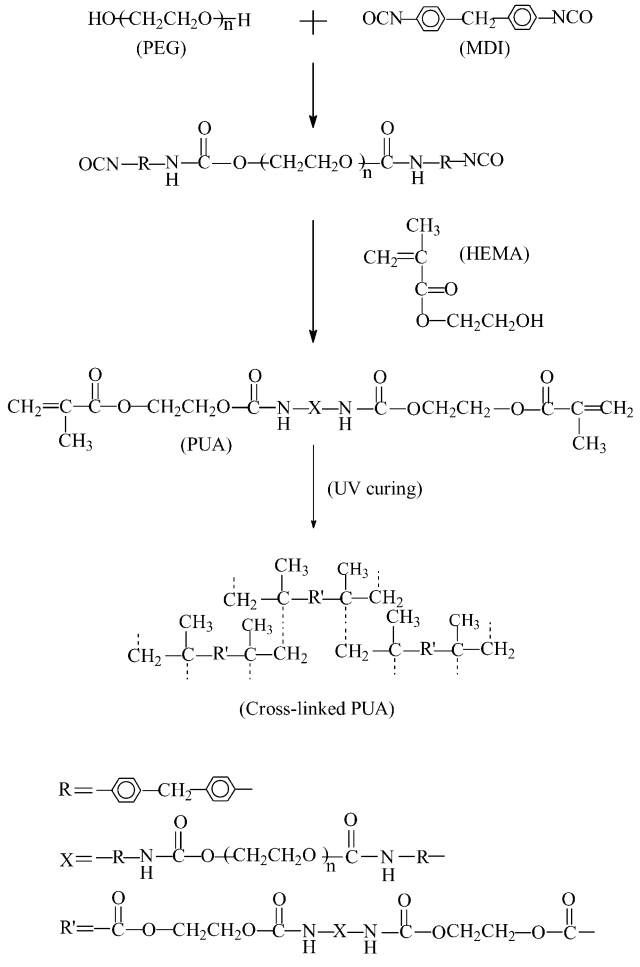

Fig. 1. Schematic representation of the synthesis of PUA.

2.3. Preparation of PUA/cross-linked PUA films and solid PEs

The PUA/cross-linked films were prepared by irradiating either PUA or a mixture of PUA and different reactive diluents (TPGDA, MMA, AN or EA) with UV radiation. The PUA was heated slightly above ambient temperature and then mixed thoroughly with different amounts of reactive diluents and 2 wt% each of benzophenone (photoinitiator, Aldrich) and *N*-methyl diethanol amine (photosensitizer, Aldrich). For irradiation, an 80 W UV lamp (365 nm) was used. Films were cast on Teflon cuvettes. The UV-cured films were then post-cured at 80 °C for 24 h. The solid PE films were also prepared in the same way, by mixing $LiClO_4$ with the PUA/diluent/photoinitiator/photosensitizer mixture before UV curing. The polymer films were designated as given in Table 1. The first two numerals after PUA indicate the weight percent of reactive diluents (T: TPGDA, M: MMA, E: EA and A: AN), and the last two numerals indicate the weight percent of the electrolytes (S: solid,

Table 1
Characterization of the PUA samples

Sample	Designation	Reactive diluent (wt%)	Electrolyte (wt%)	T_gSS[a] (°C)	T_gHS[a] (°C)
1	PUA–00–00	–	–	−20.3	43.4
2	PUA–00–S05	–	$LiClO_4$ (5)	−4.31	56.8
3	PUA–00–S10	–	$LiClO_4$ (10)	−2.59	36.4
4	PUA–00–S20	–	$LiClO_4$ (15)	−7.32	35.3
5	PUA–T05–00	TPGDA (5)	–	−19.4	58.2
6	PUA–T10–00	TPGDA (10)	–	−17.6	47.2
7	PUA–T15–00	TPGDA (15)	–	−18.5	48.7
8	PUA–T20–00	TPGDA (20)	–	−18.5	51.5
9	PUA–T25–00	TPGDA (25)	–	−14.8	45.2
10	PUA–M25–00	MMA (25)	–	−15.5	55.0
11	PUA–E25–00	EA (25)	–	−13.2	46.9
12	PUA–A25–00	AN (25)	–	−9.26	53.6
13	PUA–T05–L25	TPGDA (5)	LP-30 (25)	–	–
14	PUA–T05–L50	TPGDA (5)	LP-30 (50)	–	–
15	PUA–T05–L80	TPGDA (5)	LP-30 (80)	–	–
16	PUA–T05–L105	TPGDA (5)	LP-30 (105)	–	–
17	PUA–00–L50	–	LP-30 (50)	–	–
18	PUA–T10–L50	TPGDA (10)	LP-30 (50)	–	–
19	PUA–T15–L50	TPGDA (15)	LP-30 (50)	–	–
20	PUA–T20–L50	TPGDA (20)	LP-30 (50)	–	–
21	PUA–T25–L50	TPGDA (25)	LP-30 (50)	–	–
22	PUA–M25–L50	MMA (25)	LP-30 (50)	–	–
23	PUA–E25–L50	EA (25)	LP-30 (50)	–	–
24	PUA–A25–L50	AN (25)	LP-30 (50)	–	–

[a] The results are as available from the instrument; accuracy is +0.01 °C.

$LiClO_4$ and L: liquid, LP-30). For example, PUA–T05–L50 indicates a PUA containing 5 wt% TPGDA and 50 wt% LP-30. Weight percent was calculated based on the total weight of PUA and reactive diluents.

2.4. TGA experiment

TGA experiments were performed using a TGA 2050 instrument (TA instruments, USA) with a scan rate of 20 °C/min up to 650 °C under nitrogen atmosphere.

2.5. DSC experiment

DSC experiments were carried out using a DSC 2010 differential scanning calorimeter (TA Instruments, USA) in the temperature range of −120 to 150 °C at a scan rate of 10 °C/min. The samples were first annealed at 150 °C for 10 min, cooled down to −120 °C and then analyzed. All the thermograms reported in this study are base line corrected and calibrated against indium metal. Glass transition temperature (T_g) was reported as the midpoint of the transition process.

2.6. AC impedance measurement

Impedance measurements of the PEs were performed using UV-cured thin films made by UV curing. Film thickness was maintained in the range of 200–250 μm for the area of contact was 0.785 cm^2. For measurement of ionic conductivity, the samples were sandwiched between two stainless steel electrodes, whereas for investigation of the interfacial phenomena, the samples were sandwiched between two Li-electrodes. The electrodes were then fixed in an airtight double-wall glass cell, through the outer jacket of which thermostated water was circulated for measurements at different temperatures. Cell assembly was carried out in dry argon atmosphere inside a glove box (Vacuum Atmosphere Company, USA). Conductivity measurements were performed using an Autolab equipment (Eco Chemie B.V., The Netherlands) with PGSTAT 30 controlled by frequency response analysis system software under an oscillation potential of 10 mV. The interfacial behavior of the Li/PE/Li cell at different intervals of time was studied by AC impedance measurements under open circuit potential (OCP) condition at 25 °C.

2.7. Linear sweep voltammetry and cyclic voltammetry

Linear sweep voltammetry (LSV) and cyclic voltammetry (CV) were performed with a cell made by using stainless steel (SS 304) as working electrode and Li-metal as counter as well as reference electrode. For LSV, the potential of the working electrode was varied from 2.0 to 8.0 V (vs. Li) at a sweep rate of 5 mV/s. CV experiments were performed in the potential range of −1.0 to 4.5 V (vs. Li) at a scan rate of 5 mV/s. The electrochemical stability window and the cyclic voltammograms were obtained using an Autolab instrument (Eco Chemie B.V.,

The Netherlands) with PGSTAT 30 controlled by general purpose electrochemical system software.

3. Results and discussion

3.1. Thermal stability

The thermal stability of the undoped and doped PUAs was identified using TGA to decide on the suitability for further application in technological devices. Moreover, the high-temperature thermal event, as will be shown in DSC experiments, can also be confirmed whether it is really a phase transition or degradation associated with any weight loss. Typical TG thermograms of the undoped and doped PUA systems are shown in Fig. 2. No weight loss in the temperature region of 30–275 °C was noticed for all the samples. Fig. 2 shows that uncross-linked PUA decomposes in a single step beginning in the range of 345–370 °C. For cross-linked PUA (sample 12) containing AN as reactive diluent, the thermogram shows a two-step decomposition, where the first one starts at ~275 °C with ~25% weight loss and the second one starts at ~390 °C. The difference in the decomposition behavior of sample 12 in comparison with pure PUA may be attributed to the high reactivity of AN to generate a new phase which is rich in PAN only. As evident from Fig. 2, introduction of salt into PUA promotes the creation of a second stage beginning at 300–310 °C in all these cases, corresponding to the decomposition of the salt/polymer complex.

The thermal transition temperatures, obtained from the DSC experiments, are presented in Table 1. The DSC results of all the undoped and doped samples are characterized by two endothermic transitions. No melting transition corresponding to PEG-1000 has been observed, which indicates that the crystalline domains of PEG are destroyed at the time of cross-linking reactions. Pure PUA (without any reactive diluent) shows a low-temperature endothermic transition (T_gSS) at −20 °C and a high-temperature endothermic transition (T_gHS) at 43 °C. These two transitions correspond to the liquid–glass transition (T_g) of the amorphous regions of soft and hard segments of PUA, respectively. Addition of reactive diluents led to changes in both T_gSS and T_gHS, but no definite trend has been observed with the reactive diluent concentration. A perusal of the DSC data presented in Table 1 for the cross-linked PUA with different TPGDA contents (samples 5–9) reveals that there is no conceivable trend between T_g of the hard and soft segments of PUA units and amount of TPGDA in the blend. This may be attributed to the non-uniform cross-linking resulted in the blend with different amounts of TPGDA.

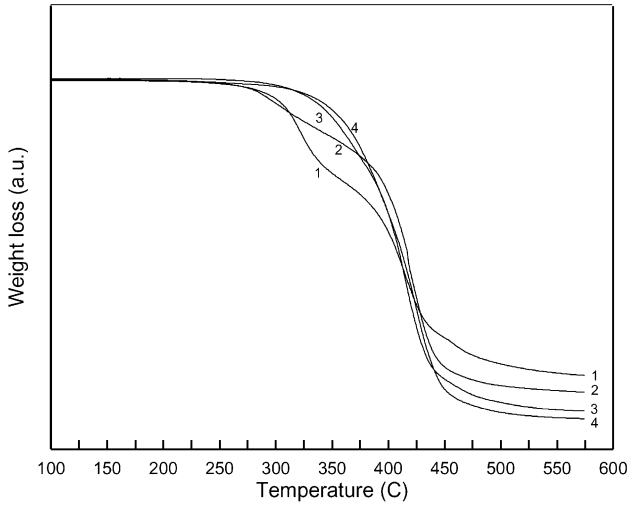

Fig. 2. Typical TG curves of some of the undoped and doped PUAs: (1) sample 2, (2) sample 12, (3) sample 9, and (4) sample 1.

Table 1 shows that both T_gSS and T_gHS undergo significant change upon addition of $LiClO_4$. Incorporation of salt into the polymer matrix leads to an increase in T_gSS. This is consistent with the previous reports [5–15] of $LiClO_4$-doped TPUs containing PEO, PPO or PTMO as soft segments. Increase in T_gSS with salt concentration indicates stiffening of the polyether chains due to the ion–dipole interactions between the Li^+ ions and the polyether oxygens. It is also evident from Table 1 that the T_gHS values tend to decrease with the increase in salt concentration. This may be due to the phase mixing of hard and soft segments in PUA in the presence of $LiClO_4$. Different types of complexes can be formed by the interaction of different coordination sites of PUA with the Li^+ ions (Fig. 3).

3.2. Ionic conductivity

The ionic conductivity (σ) was determined from the bulk resistance (R_b) which was obtained from the value of Z' at

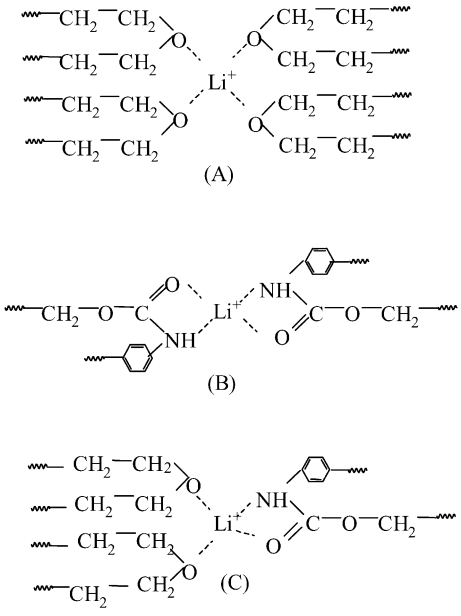

Fig. 3. Schematic representation of different complexes formed by the interaction of Li^+ with (A) polyether chains, (B) –NH and C=O groups of urethane links, and (C) both ether and urethane groups.

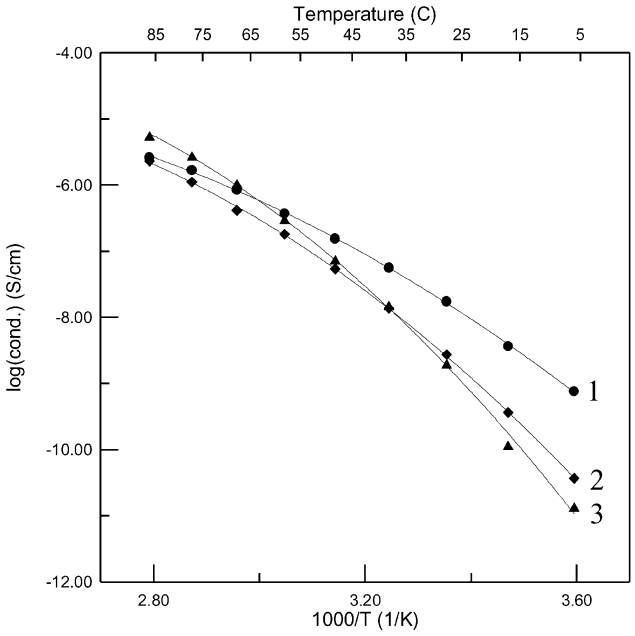

Fig. 4. Temperature dependence of ionic conductivity of PUA-doped with different amounts of $LiClO_4$: (1) sample 2, (2) sample 3, and (3) sample 4.

the minimum of jZ'' in the complex impedance plot (Z' and Z'' are the real and imaginary parts of the impedance, respectively, j is a constant) by the relationship $\sigma = l/AR_b$, where l is the thickness of the electrolyte films and A is the area of cross-section. Fig. 4 shows the ionic conductivity of PUA–$LiClO_4$-based solid electrolytes as a function of reciprocal temperature containing no reactive diluent and having different concentrations of $LiClO_4$. It is evident from Fig. 4 that the variation of conductivity with reciprocal temperature follows Vogel–Tamman–Fulcher (VTF) relationship (Eq. (1)), which suggests that the ion transport is coupled with the polymer segmental motion

$$\sigma(T) = AT^{-1/2} \exp[-B/k_B(T - T_0)] \quad (1)$$

where A is a constant proportional to the number of charge carriers, B is the pseudo-activation energy related to polymer segmental motion, k_B is the Boltzmann constant, and T_0 is a reference temperature usually associated with the

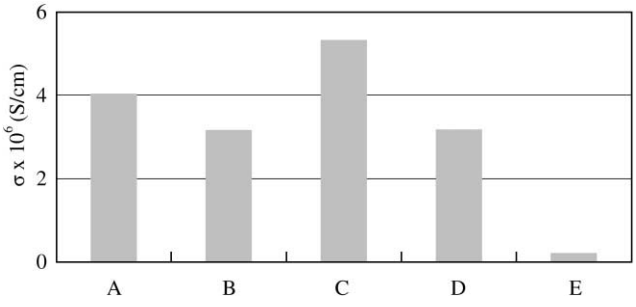

Fig. 5. Ionic conductivity of PUA cross-linked with different reactive diluents at 25 °C: (A) sample 17, (B) sample 21, (C) sample 22, (D) sample 23, and (E) sample 24.

ideal T_g at which free volume disappears or the temperature at which the configurational entropy becomes zero. It is to be noted that the relationship of conductivity with salt concentration is a complex one. At low-temperature region, higher salt-containing electrolytes have lower conductivity, whereas at high-temperature region, the reverse relationship is observed. Samples containing higher amount of salt contain higher number of charge carriers, but the T_g of the complex is simultaneously increased with the increasing salt concentration. Increase in T_g leads to a decrease in segmental motion and hence the ionic mobility. Hence, at low-temperature region, the samples containing higher amount of salt, though containing higher amount of charge carriers, show lower conductivity as the mobility is restricted. Another possibility is the increase in ion pair formation with the increasing salt concentration [25]. At higher temperature, the mobility of the charge carriers is increased as the polymer segmental motion is increased, and hence the reverse relationship between conductivity and salt concentration is observed. Moreover, the number of charge carriers is known to be temperature dependent [8]. Hence, the increase in temperature will lead to an increase in the number of charge carriers by the dissociation of some of the ion pairs.

Fig. 5 shows the effect of reactive diluents on the conductivity of the cross-linked electrolytes at 25 °C containing 25 wt% of each of the reactive diluents and 50 wt% of LP-30. Ionic conductivity of all the samples is in the range of 10^{-6} S/cm at 25 °C except sample 24 containing AN as reactive diluent, which shows conductivity of the order of 10^{-7} S/cm. The lower conductivity of sample 24 might be associated with the comparatively higher T_g of the soft segment of sample (see sample 12, Table 1). Sample 22 (containing MMA as diluent) shows highest conductivity, but the stability of sample 22 (and also sample 23) is comparatively poor. These samples swell very fast in LP-30 and become soft on prolonged exposure. Samples containing TPGDA as reactive diluent show excellent stability in LP-30. No deterioration of mechanical properties could be noticed even after 7 days exposure to LP-30. The higher stability of TPGDA-containing samples is associated with the presence of two double bonds in TPGDA molecule that can enhance cross-linking. TPGDA is, therefore, chosen as the reactive diluent for cross-linking and subsequent preparation of PEs for our further studies.

Fig. 6 shows the variation of conductivity at 25 °C with TPGDA content of the electrolytes. All the samples contain 50 wt% of LP-30. It is evident from Fig. 6 that the conductivity is decreased to a plateau with the increase in TPGDA content. Increase in TPGDA content leads to an increase in the cross-link density of the electrolytes, which decreased the segmental motion of the polymer chains. However, in gel electrolytes, the role of the polymer is believed to hold the liquid electrolyte, and the ions are transported through the plasticizer solvent. If this is the case, then there should not be any decrease in conductivity with the increase in

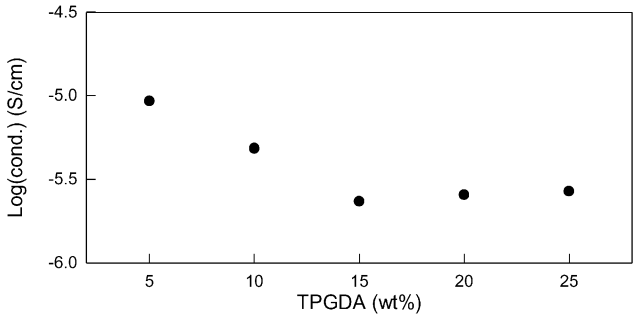

Fig. 6. Variation of ionic conductivity of PUA (containing 50 wt% LP-30) with TPGDA content at 25 °C.

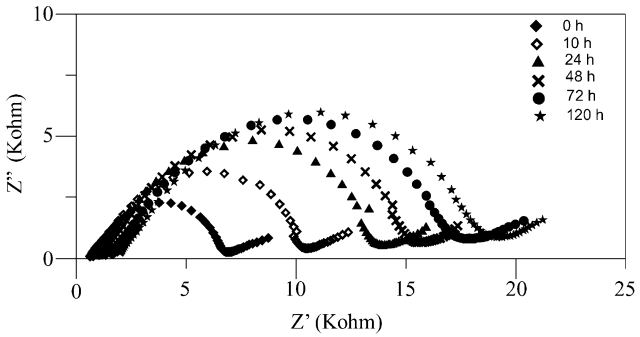

Fig. 8. Time evolution AC impedance spectra of a Li/PE(sample 15)/Li cell at 25 °C.

cross-link density of the polymers. In this study, the lower concentration of LP-30 (50 wt%) might be the reason for such behavior. As will be seen later (Fig. 7), there is a transition from VTF to Arrhenius behavior of conductivity with temperature at higher concentration of LP-30. Hence, it is reasonable to accept that at lower concentration of LP-30, the ion movement is partly influenced by the polymer segmental motion.

Addition of TPGDA increases the mechanical property and the stability of the polymers in liquid electrolytes, but at the expense of the ionic conductivity. We, therefore, optimized the TPGDA content at 5 wt% in order to have a compromise between ionic conductivity and mechanical property of the electrolytes. The ionic conductivity of the gel electrolytes containing 5 wt% TPGDA and different concentrations of LP-30 is presented in Fig. 7. It has been observed that the ionic conductivity of the gel electrolytes is increased with the increase in temperature following the VTF relationship. At higher concentrations of LP-30 (samples 15 and 16), the plot of log σ vs. 1000/T becomes close to a linear one, which is best described by the Arrhenius equation (Eq. (2))

$$\sigma(T) = A \exp[-E/k_B T] \quad (2)$$

where A is a constant proportional to the number of charge carriers, E is the activation energy and k_B is the Boltzmann constant. Arrhenius relationship is valid when the ion movement is decoupled from the polymer segmental motion. When the liquid concentration is low, the ions are not fully decoupled from the polymer segmental motion, whereas at higher liquid electrolyte concentration, the ions are completely decoupled from the polymer segmental motion. Hence, there is a transition from VTF to Arrhenius behavior at higher liquid electrolyte concentration.

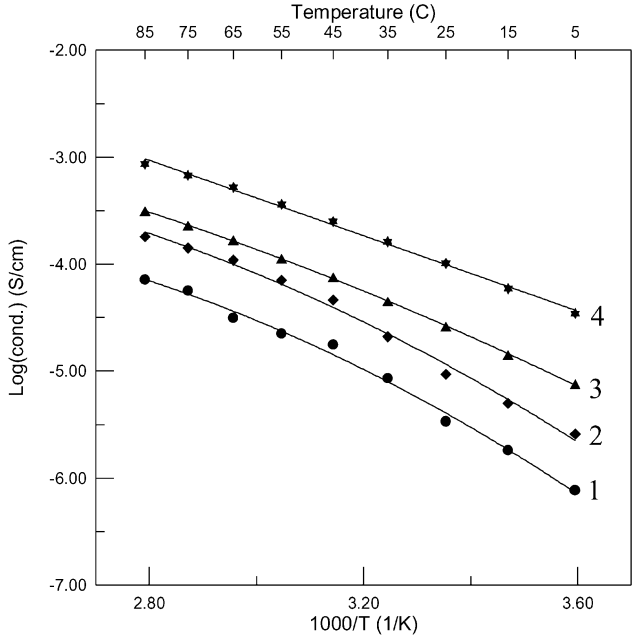

Fig. 7. Temperature dependence of ionic conductivity of (1) sample 13, (2) sample 14, (3) sample 15, and (4) sample 16.

3.3. Interfacial behavior

For successful performance of a PE in Li-batteries, good compatibility of the electrolyte with Li-metal is essential. Here, we attempted to investigate the interfacial behavior of PUA cross-linked with TPGDA in contact with Li-electrodes under prolonged exposure in order to check their compatibility with Li-electrodes. For this purpose, AC impedance of Li/PE/Li cell under open-circuit conditions has been measured at different intervals of time. Fig. 8 shows the time evolution response of AC impedance of sample 15 at 25 °C. From these AC impedance spectra, it is possible to calculate the electrolyte resistance (R_e) and the interfacial resistance (R_i). The electrolyte resistance is the intercept on the real axis of the high-frequency side of the spectra, whereas the intercept on the low-frequency side indicates ($R_e + R_i$). Fig. 8 shows that there is a progressive expansion of the high-frequency semicircle indicating an increase in ($R_e + R_i$) with time. Variation of R_e and R_i with time is presented in Fig. 9. It is to be noted that the electrolyte resistance has a slight increasing trend with time. Such fluctuation of R_e with time may be the consequence of loss of the solvent by means of evaporation, reaction with Li, etc.

The interfacial resistance of Li/PE/Li cell is found to

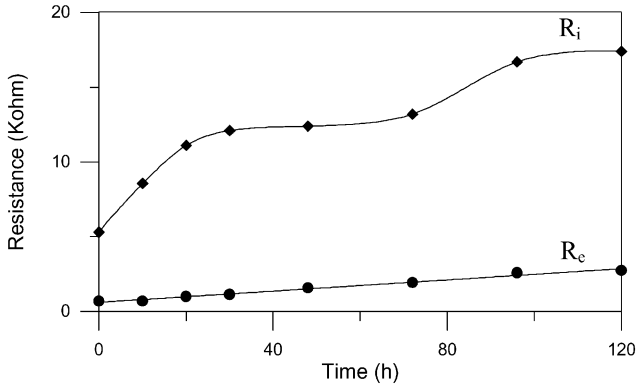

Fig. 9. Variation of R_e and R_i of the Li/PE(sample 15)/Li cell with storage time at 25 °C.

increase initially and then it tends to stabilize with time. The initial increase of R_i may be attributed to the formation of a passive layer due to the reaction of the electrolyte with Li-metal. Considering the intrinsic stability of the polymer backbone, one might speculate that Li-metal reacts with the carbonated solvents EC/DMC of the liquid electrolyte. Carbonated solvents like EC/DMC/PC are well known to react with Li-metal [26,27] and consequently passivate the Li-electrodes. The tendency of R_i to attain a steady state with time indicates the absence of further growth of the passive layer. This result indicates a good compatibility of PUA with the liquid electrolytes, which reduces the affinity of the liquid electrolyte to the Li-electrodes.

3.4. Electrochemical stability

In order to ascertain the electrochemical stability of the PUA electrolytes, LSV experiments were performed on the laminated three electrode cells at ambient temperature. The linear sweep voltammograms of sample 15 are presented in Fig. 10. The working electrode potential of the cell was varied from 2.0 to 7.0 V (vs. Li) at a sweep rate of 5 mV/s. It is evident from Fig. 10 that there is no electrochemical reaction in the potential range 2.0–4.8 V.

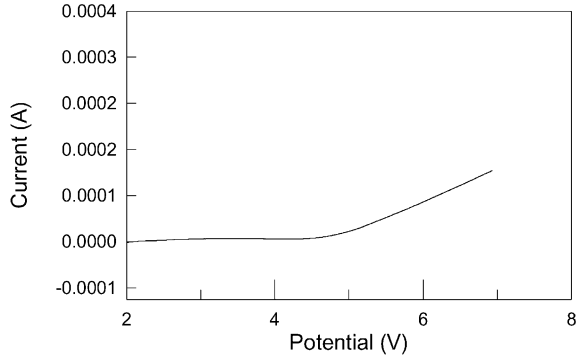

Fig. 10. Electrochemical stability window of sample 15 performed by LSV method.

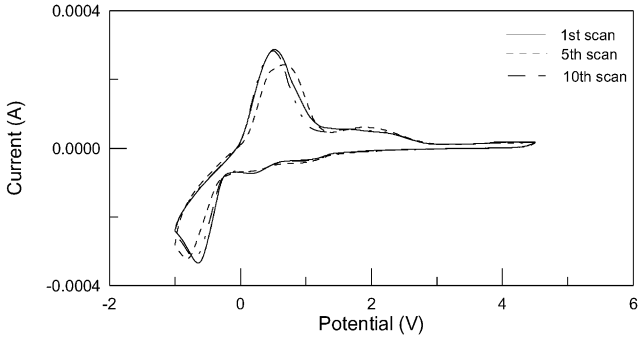

Fig. 11. Cyclic voltammograms of the Li/PE(sample 15)/SS cell at ambient temperature.

The onset of current flow at 4.8 V is associated with the decomposition of the electrolyte. The anodic stability limit of the electrolyte (4.8 V) is comparable to the PAN-based (4.3–5.0 V) [28] and PMMA-based gel electrolytes (4.5–4.8 V) [29].

CV was performed to study the kinetics of Li deposition–stripping process. Fig. 11 shows the cyclic voltammograms for the Li/PE/SS three electrode cell using sample 15 at ambient temperature. On sweeping cathodically, a cathodic peak is observed at ~ -0.61 V, which corresponds to the deposition of Li on the SS electrode. On the reverse scan, stripping of Li is observed at ~0.52 V. It is evident from Fig. 11 that the Li deposition–stripping process is reversible and there is no other oxidation peak up to 4.5 V. This indicates that the cross-linked PUA system is electrochemically stable up to a potential of 4.50 V. Hence, it can be safely used as PE in rechargeable Li-batteries.

4. Conclusion

The ionic conductivity and electrochemical properties of a series of cross-linked PUA electrolytes, plasticized with LP-30, have been investigated and compared with parent PUA (without any reactive diluent). The ionic conductivity and also the mechanical properties of the cross-linked PUA-based electrolytes were found to depend on the type of reactive diluents used for cross-linking. Of the different types of reactive diluents used, MMA exhibited higher ionic conductivity than the others, but this system is not very much stable in LP-30. The TPGDA cross-linked system showed a good combination of conductivity and mechanical properties. One of the plasticized PEs studied in this work exhibited ionic conductivity as high as 1.01×10^{-4} S/cm at 25 °C. These electrolytes showed good compatibility with Li-electrodes and sufficient electrochemical stability (up to 4.8 V vs. Li) for safe operation in Li-batteries.

Acknowledgements

The financial support of this work by the National

Science Council of Taiwan under projects NSC 88-2622-E006-008 and NSC 89-2622-E006-001 is gratefully acknowledged.

References

[1] MacCallum JR, Vincent CA, editors. Polymer electrolyte reviews 1 & 2. London: Elsevier, 1987–1989.
[2] Gray FM, editor. Solid polymer electrolytes—fundamental and technological applications. Weinheim: VCH, 1991.
[3] Scrosati B, editor. Application of electro-active polymers. London: Chapman & Hall, 1993.
[4] LeNest JF, Gandini A, Cheradame H. Br Polym J 1986;20:253.
[5] McLennaghan AW, Pethrick RA. Eur Polym J 1988;24:1063.
[6] McLennaghan AW, Hooper A, Pethrick RA. Eur Polym J 1989;25:1297.
[7] Watanabe M, Oohashi S, Sanui K, Kobayashi T, Ohtaki Z. Macromolecules 1985;18:1945.
[8] Watanabe M, Sanui K, Ogata N. Macromolecules 1986;19:815.
[9] van Heumen JD, Stevens JR. Macromolecules 1995;28:4268.
[10] Seki M, Sato K. Makromol Chem 1992;193:2971.
[11] Ferry A, Jacobson P, van Heumen JD, Stevens JR. Polymer 1996;37:737.
[12] Ng STC, Forsyth M, Macfarlane DR, Garcia M, Smith ME, Strange JH. Polymer 1998;39:6261.
[13] Furtado C, Goulart Silva G, Machado JC, Pimenta MA, Silva RA. J Phys Chem B 1999;103:7102.
[14] Wang HL, Kao HM, Digar ML, Wen TC. Macromolecules 2001;34:529.
[15] Digar ML, Hung SL, Wang HL, Wen TC, Gopalan A. Polymer, in press.
[16] Mocanin J, Cuddihy EF. J Polym Sci C 1966;14:313.
[17] Santaniello E, Manzocchi A, Sozzani P. Tetrahedron Lett 1979;47:4581.
[18] Blonsky PM, Shriver DF, Austin P, Allcock HR. J Am Chem Soc 1984;106:6854.
[19] Blonsky PM, Shriver DF, Austin P, Allcock HR. Solid State Ion 1986;18/19:258.
[20] Tonge JS, Shriver DF. J Electrochem Soc 1987;134:269.
[21] Bennett JL, Dembek AA, Allcock HR, Heyen BJ, Shriver DF. Chem Mater 1989;1:14.
[22] Velankar S, Pazos J, Cooper SL. J Appl Polym Sci 1996;62:1361.
[23] Allen NS, Johnson MS, Oldring PKT, Salim S. In: Oldring PKT, editor. Chemistry and technology of UV and EB formulations for coatings, inks and paints, vol. 1. London: SITA, 1991. p. 115.
[24] Kim CS, Kim BH, Kim K. J Power Sour 1999;84:12.
[25] Schantz S, Torrell LM, Stevens JR. J Chem Phys 1991;94:6862.
[26] Thevenin JG, Muller RH. J Electrochem Soc 1987;134:273.
[27] Aurbach D, Weissman I, Zaban A, Chusid O. Electrochim Acta 1994;39:51.
[28] Croce F, Gerace F, Dantzemberg G, Passerini S, Appetecchi GB, Scrosati B. Electrochim Acta 1994;39:2187.
[29] Appetecchi GB, Croce F, Scrosati B. Electrochim Acta 1995;40:991.